AIP | Applied Physics Letters

Fe/MgO/Fe (100) textured tunnel junctions exhibiting spin polarization features of single crystal junctions

A. Duluard, B. Negulescu, C. Bellouard, M. Hehn, D. Lacour et al.

Citation: Appl. Phys. Lett. **100**, 072408 (2012); doi: 10.1063/1.3687174
View online: http://dx.doi.org/10.1063/1.3687174
View Table of Contents: http://apl.aip.org/resource/1/APPLAB/v100/i7
Published by the American Institute of Physics.

Fe/MgO/Fe (100) textured tunnel junctions exhibiting spin polarization features of single crystal junctions

A. Duluard,[1] B. Negulescu,[2] C. Bellouard,[1] M. Hehn,[1] D. Lacour,[1] Y. Lu,[1] G. Lengaigne,[1] F. Montaigne,[1] S. Robert,[1] S. Suire,[1] and C. Tiusan[1,3,a)]
[1]*Institut Jean Lamour, CNRS—Nancy Université, BP 70239, F–54506 Vandoeuvre, France*
[2]*LEMA, UMR 6157 CNRS-CEA, Université François Rabelais Tours, Parc de Grandmont, 37200 Tours, France*
[3]*Materials Science Laboratory, Technical University of Cluj-Napoca, Cluj-Napoca, Romania*

(Received 28 November 2011; accepted 1 February 2012; published online 17 February 2012)

Crystallographic and spin polarized transport properties of (100) textured and (100) epitaxial Fe/MgO/Fe magnetic tunnel junctions are compared. Strong similarities in the transport properties show that structural coherence and magnetic quality at the 25 nm grain scale in textured junctions are sufficient to issue signatures of the spin polarized transport specific to a single crystal junction. This demonstrates that the lateral coherence of the Bloch tunneling wave function is identically limited in both systems. Our analysis leads to model the textured tunnel junction as a juxtaposition of nanometer sized single crystal junctions, placed in parallel. © *2012 American Institute of Physics*. [doi:10.1063/1.3687174]

Since the discovery of the tunneling magnetoresistance (TMR) effect in epitaxial magnetic tunnel junctions (MTJs), the (100) Fe/MgO/Fe system has been considered to be a model system for studies of spin dependent tunneling (SDT). Extending from the fundamental discoveries of Julliere[1] and Moodera[2] in amorphous oxide magnetic tunnel junctions, a more complete picture of SDT has been formulated in single crystal MTJs by taking into account the symmetry dependent filtering, which should ensure very high TMR ratios. However, the predicted TMR ratios[3] have thus far not been realized experimentally.[4] Structural (i.e., misfit dislocations) and/or chemical imperfections, which are detrimental to symmetry filtering effects, are commonly suspected to be the primary limiting factors in high TMR ratios in single crystal MTJs.[5,6]

On the other hand, textured CoFeB/MgO/CoFeB MTJs grown by sputtering show high TMR ratios, of over 1100% at 5 K, and whose characteristics signify the presence of symmetry dependent filtering.[7] A larger TMR ratio is expected in these systems because the tunneling polarization provided by the (100) bcc CoFe is larger than the one of the (100) bcc Fe. Yet the effect of texturing should result in a lowered TMR ratio due to the reduction of the lateral structural coherence by the presence of numerous defects such as grain boundaries in the barrier and the electrodes.

In order to better understand the relationship between polycrystalline structure and TMR and/or transport mechanisms, we present a comparative SDT analysis in single crystal and textured Fe/MgO/Fe MTJs grown in similar conditions. This study will demonstrate that the textured MTJ behaves like an assembly of nanometer-sized single crystal junctions without any contribution from grain boundaries. This result provides a new insight for understanding the unexpectedly highly spin-polarized transport in textured MTJs with CoFeB electrodes.

Single crystal (SC) and textured (T) MTJs have been grown on different substrates. The SC sample (Fe 45 nm/MgO/Fe 10 nm/Co 20 nm/Au 20 nm) was grown on a (100) MgO single crystal substrate. Details on physical properties and device fabrication can be found elsewhere.[6,8] The T sample (Fe 30 nm/MgO/Fe 10 nm/Co 30 nm/Au 20 nm) was deposited on (100) Si substrate coated by a 5 nm thick MgO film in a separate sputtering plant. Due to the 22.5% lattice mismatch, the growth of (100) epitaxial MgO on Si is challenging. Different preparation methods have been reported in Refs. 9 and 10. In our study, the Si substrate natively oxidized is etched using a 100 W RF Ar plasma under a pressure of 10^{-2} mbar and coated by MgO. Afterwards, both samples are grown by molecular beam epitaxy (MBE) in a chamber with a base pressure of 5×10^{-11} Torr, and equipped with *in-situ* reflection high energy electron diffraction (RHEED) facilities.

Our RHEED analysis (Figs. 1(a)–1(d)) provides comparative information on the structural properties of the Fe layer which forms the bottom electrode in both junctions. The as-deposited Fe on the Si/MgO substrate has a polycrystalline structure with traces of the (100) texture (Fig. 1(a)). After 20 min of annealing at 500 °C, the crystalline structure of the Fe film is vastly improved and displays a highly textured (100) structure (Fig. 1(b)). These two RHEED diffraction patterns are independent on the incident electron's direction and simultaneously exhibit the characteristic [01] and [11] rods of the single crystal Fe surface lattice (Figs. 1(c) and 1(d)). Further structural analysis has been performed *ex-situ* by x-ray diffraction (XRD) in samples where the 30 nm thick Fe textured layer was capped with a 3 nm MgO layer. The diffraction pattern shows only the (100) peaks of the Fe layer and Si substrate, validating once more the highly (100) textured growth of the Fe layer. Moreover, from the in-plane XRD analysis, we used Scherrer's formula to calculate an average size of the Fe grains of about 25 nm. The flat SC Fe surface allows the observation of RHEED intensity oscillations during the complete growth process of the MgO barrier

a)Electronic mail: coriolan.tiusan@phys.utcluj.ro.

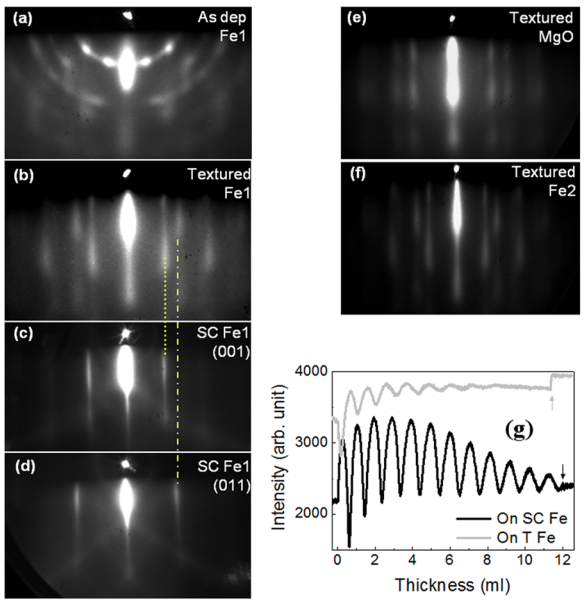

FIG. 1. (Color online) RHEED diffraction patterns of: (a) as deposited in-plane isotropic 30 nm Fe on MgO/Si substrate; (b) textured Fe film after annealing at 500 °C for 20 min; (c) (001) direction and (d) (011) direction of SC Fe film grown on MgO substrate; (e) MgO textured barrier; (f) top textured Fe layer after 10 min annealing at 350 °C; and (g) RHEED oscillations for the MgO barrier deposition for the SC (black) and the textured (gray) sample MTJ.

(Fig. 1(g)) and, therefore, precise control of the deposition of 12 monolayers (ML). Contrast this with the T sample, whose top surface exhibits much higher roughness characteristics, as shown in the RHEED pattern (Fig. 1(b)): lower contrast (larger diffuse background) and higher order diffraction spots. Nevertheless, the surface is sufficiently flat within the RHEED coherence length scale to observe intensity oscillations during the growth of the first MgO layers (Fig. 1(g)). The nominal thickness of the MgO barrier has then been evaluated to 11.5 ± 0.5 ML. These thicknesses are in agreement with the respective product of resistance and area (RA) of the junctions measured at 10 K in parallel (P) configuration: $1.1 \times 10^6\ \Omega\ \mu m^2$ (T) and $1.6 \times 10^6\ \Omega\ \mu m^2$ (SC). The MgO epitaxy on the textured Fe layer is confirmed by the perfect similitude of the texture (Fig. 1(e)) with respect to the bottom textured electrode (Fig. 1(b)). The top Fe electrode of the MTJ, epitaxially grown on the textured barrier, follows the growing template imposed by the underlying structure. Its crystalline quality has been improved by annealing at 350 °C for 10 min (see Fig. 1(f)). A so-called "grain to grain epitaxy[11]" is then directly achieved during the growth. This results in a columnar structure similar to what is achieved by *ex-situ* annealing in CoFeB/MgO/CoFeB MTJs, where the MgO crystalline surface acts as a crystallization template for CoFeB electrodes.[11] Finally, as for SC MTJ, the top Fe layer is magnetically hardened by a Co layer, with the entire stack capped by a Au layer.

Electrical characterization was completed on 10–40 μm square MTJs patterned by a combined UV lithography/ion etching process. The TMR loops (R(H)) of the SC exhibit a four-fold anisotropy with a saturated 150% TMR ratio along the easy axis (Fig. 2(a)) and 140% along the hard axis. Even though no well defined plateau is observed for the T junction (Fig. 2(b)), the TMR is slightly reduced (130%), in any arbi-

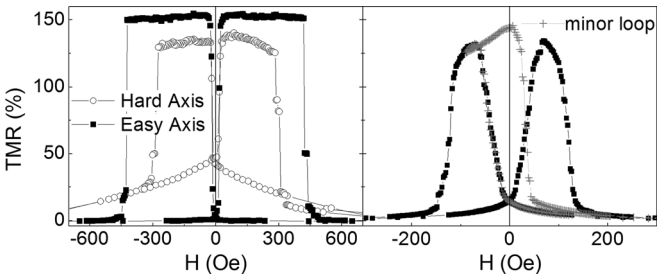

FIG. 2. TMR(H) loops for epitaxial (a) and textured (b) MTJ. For the textured MTJ, all the in-plane directions are magnetically equivalent (isotropic R(H) curves).

trary magnetic field orientation. A maximum TMR value of 140% is even reached at zero field in the minor loop (Fig. 2(b)). This demonstrates that the best antiparallel (AP) configuration of the electrodes is obtained when the magnetization direction of the grains is governed by the local crystalline axis, without any applied field. Moreover, this result indicates the presence of perpendicular structural and corresponding magnetic coherence across the stack, at the scale of a grain. Each grain constitutes a perpendicular MTJ pillar with well defined P and AP magnetic configurations, with in-plane randomly distributed anisotropy axis from one grain to the other.

Figures 3(a)–3(d) show the bias dependence of the TMR at 10 K and of the tunneling conductivity ($G = dI/dV$) in the P or AP magnetization configurations at 300 K and 10 K for both samples. For comparison between samples, the P and AP conductances of the T junction were multiplied by a given factor. This factor was established by superimposing the AP conductances at 10 K of the SC and T junctions at zero bias (Fig. 3(b)). Thus, the bias dependences of G_{AP} for

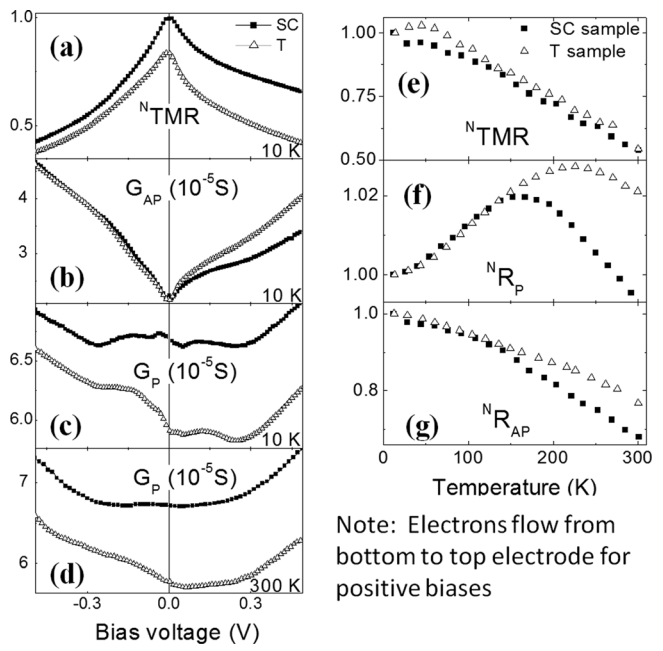

FIG. 3. For SC and T MTJs bias dependence of: (a) TMR at 10 K, normalized with respect to the maximum value of the SC junction; (b) conductance at 10 K in AP configuration; (c) conductance at 10 K in P configuration; (d) conductance at 300 K in parallel configuration; and (e)–(g) temperature dependence of the normalized TMR ratio, ^{N}TMR, and of the P and AP resistances, $^{N}R_P$ and $^{N}R_{AP}$ measured at 10 mV, with respect to their low temperature values.

negative voltage are exactly superimposed. Moreover, we point out that the other parameters, TMR or G_P exhibit very close bias dependence in this negative voltage range corresponding to electrons injected from top to bottom electrode. This is consistent with very similar structural quality and electronic structure of the bottom electrode in both samples. On the other hand, the main shift between both samples for all parameters is observed when the voltage is increased towards positive values, when the electrons are injected to the top electrode. As shown by RHEED oscillations during the barrier growth, the MgO barrier and then the top electrode of T sample have distinctly different structural properties relative to SC. This induces a loss of symmetry filtering and then an increase of G_{AP} and a decrease of G_P in positive bias with respect to the conductances of the SC reference (Figs. 3(b) and 3(c)). As a matter of fact, the TMR of T junction (Fig. 3(a)) is almost symmetric, as observed in polycrystalline junctions. Nevertheless, Figures 3(c) and 3(d) show that $G_P(V)$ presents minima for the same biases in both samples. Especially at 10 K, the inflection points are similar in number and position. In particular, $G_P(V)$ exhibits a local minimum around ± 0.2 V for both samples. It is commonly attributed to symmetry dependent tunneling, namely the signature of the Δ_5 symmetry conduction channel contribution.[6] Moreover, the $G_{AP}(V)$ measured at 10 K in Figure 3(c) shows for both samples the specific electronic structure signature at low bias related to the minority spin surface state of (100) Fe (inflection point in G_{AP} around 0.2 eV).[6]

The temperature dependences of the TMR ratio and of the P and AP resistances are presented in Figures 3(e)–3(g). Similar behavior is qualitatively observed in both samples for the three parameters. The TMR(T) curves of both samples are perfectly superimposed. The TMR ratio roughly doubles between room temperature and 10 K, as commonly observed in epitaxial Fe/MgO within the same MgO thickness range.[12] The AP resistance increases significantly with decreasing temperature as expected for tunneling transport, while only a small non-monotonic variation of R_P is measured. $R_P(T)$ indeed presents a maximum in both samples and decreases similarly with decreasing temperature below 150 K. This behavior is non-conventional with respect to free electron tunneling. Nevertheless, it has already been observed in mono-crystalline junctions and is considered as a criterion of high quality samples where symmetry filtering effects are observed.[12,13] This has been attributed to a spin-flip scattering mechanism by Ma *et al.*[12] However, Lu *et al.* suggest that the experimental absence of magnon related features in dI^2/dV^2 curve in P state requires that this effect be understood through symmetry dependent interface diffusion due to the presence of spin polarized interface states.[13] Finally, at temperatures above 250 K, concerning the expected decrease of resistance with temperature, the textured MTJ shows a smaller R(T) slope both in P and AP configurations. This single difference between both samples, which does not affect the temperature dependence of the TMR ratio, can be attributed to a lower barrier thickness of the T sample, in agreement with the RA product values. Qualitatively, the same tendency has been observed by Ma *et al.* with varying MgO thicknesses roughly from 7 to 14 ML.[12] In this reference, for thicker barriers, the AP resistance presents indeed a steeper temperature variation with respect to its low temperature value.

In conclusion, high quality textured Fe/MgO/Fe tunnel junctions have been grown on (100) Si substrate. Their transport properties exhibit the voltage and temperature response of single crystal junctions, without any contributions from grain boundaries. The textured MTJs can then be modeled as a network of approximately 25 nm lateral size epitaxial MTJs, whereby this network is characterized by in-plane randomly disordered single crystal grains. The similarities in the transport characteristics for single crystal and textured Fe/MgO/Fe junctions suggest that the lateral coherence of the Bloch wave function is reduced in both cases by the dislocations network within the MgO. The misfit of the lattice parameter with Fe (3.7%) leads indeed to a dislocation period around 5 nm in a single crystal junction.[5,6] Therefore, our study demonstrates that, from the spin and symmetry filtering effects point of view, single crystal and textured MTJs are equivalent. This is very important for technological applications that would want to utilize sputtering growth techniques in the fabrication of spintronic devices. Moreover, our study offers new arguments for the comparison with the sputtered CoFeB/MgO/CoFeB MTJs. As proposed by Choi *et al.*,[11] in these systems, the coherent tunneling seems to be expanded to the size of a grain. The MgO initially grows on amorphous CoFeB, and therefore, no initial strains/dislocations within the MgO are expected. A segregation of boron at the interface with MgO has been observed in these systems after the annealing and crystallization stages.[14,15] A high concentration of B near the interface could help the matching between MgO and Fe lattices during the annealing and crystallization processes. Besides any electronic structures aspects (enhanced polarization of CoFe with respect to Fe), absence or a larger period of dislocation network would furthermore explain larger spin filtering efficiency and corresponding TMR effects in CoFeB/MgO/CoFeB MTJs.

C. Tiusan acknowledges the SPINCHAT project ANR-07-BLAN-341 and POS CCE ID. 574, code SMIS-CSNR 12467.

[1]M. Julliere, Phys. Lett. A **54**, 225 (1975).
[2]J. S. Moodera, L. R. Kinder, T. M. Wong, and R. Meservey, Phys. Rev. Lett. **74**(16), 3273 (1995).
[3]W. H. Butler, X.-G. Zhang, T. C. Schulthess, and J. M. MacLaren, Phys. Rev. B **63**, 054416 (2001); J. Mathon and A. Umerski, *ibid.* **63**, 220403 (2001).
[4]S. Yuasa, T. Nagahama, A. Fukushima, Y. Suzuki, and K. Ando, Nature Mater. **3**, 868 (2004).
[5]F. Bonell, S. Andrieu, F. Bertran, P. Lefevre, A. T. Ibrahimi, E. Snoeck, C. Tiusan, and F. Montaigne, IEEE Trans. Magn. **45**, 3467 (2009).
[6]C. Tiusan, M. Hehn, F. Montaigne, F. Greullet, S. Andrieu, and A. Schuhl, J. Phys.: Condens. Matter **19**, 165201 (2007).
[7]S. Ikeda, J. Hayakawa, Y. Ashizawa, Y. Lee, K. Miura, H. Hasegawa, M. Tsunoda, F. Matsukura, and H. Ohno, Appl. Phys. Lett. **93**, 082508 (2008).
[8]J. Faure-Vincent, C. Tiusan, E. Jouguelet, F. Canet, M. Sajieddine, C. Bellouard, E. Popova, M. Hehn, F. Montaigne, and A. Schuhl, Appl. Phys. Lett. **82**, 4507 (2003).
[9]G. X. Miao, J. Y. Chang, M. J. van Veenhuizen, K. Thiel, M. Seibt, G. Eilers, M. Münzenberg, and J. S. Moodera, Appl. Phys. Lett. **93**, 142511 (2008); M. Ning, Y. Y. Mi, C. K. Ong, P. C. Lim, and S. J. Wang, J. Phys. D: Appl. Phys. **40**, 3678 (2007).
[10]A. Kohn, A. Kovács, T. Uhrmann, T. Dimopoulos, and H. Brückl, Appl. Phys. Lett. **95**, 042506 (2009).

[11]Y. S. Choi, K. Tsunekawa, Y. Nagamine, and D. Djayaprawira, J. Appl. Phys. **101**, 013907 (2007).
[12]Q. L. Ma, S. G. Wang, J. Zhang, Y. Wang, R. C. C. Ward, C. Wang, A. Kohn, X.-G. Zhang, and X. F. Han, Appl. Phys. Lett. **95**, 052506 (2009).
[13]Y. Lu, H. X. Yang, C. Tiusan, M. Hehn, M. Chshiev, C. Bellouard, B. Kierren, G. Lengaigne, A. Duluard, D. Lacour *et al.*, "Symmetry dependent scattering by minority interface resonance states in single-crystal magnetic tunnel junctions," Phys. Rev. Lett. (submitted).
[14]S. Pinitsoontom, A. Cerezo, A. K. Petford-Long, D. Mauri, L. Folks, and M. J. Carey, Appl. Phys. Lett. **93**, 071901 (2008).
[15]C. Y. You, T. Ohkubo, Y. K. Takahashi, and K. Hono, J. Appl. Phys. **104**, 033517 (2008).